

Original Article

Upregulation of CENPM facilitates lung adenocarcinoma progression via PI3K/AKT/mTOR signaling pathway

Chao Liu^{1,†}, Yun Wang^{1,†}, Yuyang Dao¹, Shuting Wang², Fei Hou¹, Zhixian Yang¹, Pengjie Liu¹, Juan Lv¹, Ling Lv¹, Gaofeng Li^{2,*}, Youjun Zhou^{3,*}, and Zhiyong Deng^{1,*}

¹Department of Nuclear Medicine, Tumor Hospital of Yunnan Province, the Third Affiliated Hospital of Kunming Medical College, Kunming 650118, China, ²Department of Thoracic Surgery, Tumor Hospital of Yunnan Province, the Third Affiliated Hospital of Kunming Medical College, Kunming 650118, China, and ³Department of Nuclear Medicine, the Affiliated Yan'an Hospital of Kunming Medical College, Kunming 650118, China

[†]These authors contributed equally to this work.

*Correspondence address. Tel: +86-13987123539; E-mail: ligaofeng1965@163.com (G.L.) / E-mail: zhouyoujun122@163.com (Y.Z.) / E-mail: 13888158986@163.com (Z.D.)

Received 21 June 2021 Accepted 29 August 2021

Abstract

Centromere protein M (CENPM) is essential for chromosome separation during mitosis. However, its roles in lung adenocarcinoma (LUAD) progression and metastasis remain unknown. In this study, we aimed to explore the effects of CENPM on LUAD progression as well as the underlying mechanisms. We analyzed the expression of CENPM and its correlation with clinicopathological characteristics using GEO LUAD chip datasets and TCGA dataset. We further investigated the impact of CENPM on LUAD *in vitro* and *in vivo*. *In silico* analysis and qRT-PCR revealed that CENPM is upregulated in LUAD compared with that in normal lung tissues. Via gain/loss-of-function assays, we further found that CENPM promotes the LUAD cell cycle, cell proliferation, migration and invasion, and inhibits cell apoptosis *in vitro*. The *in vivo* study showed that loss of CENPM inhibits the growth of A549 xenografts. Furthermore, we found that CENPM can promote the phosphorylation of mTOR rather than directly affect the mTOR content. Inhibition of mTOR activity abrogates the promoting effects of CENPM on cell cycle progression, cell proliferation, migration and invasion. Taken together, these results show that CENPM plays an important role in the growth and metastasis of LUAD and may be a promising therapeutic target in LUAD.

Key words CENPM, lung adenocarcinoma, PI3K/AKT/mTOR signaling pathway

Introduction

Lung cancer, a malignant tumor with the highest morbidity in humans, is the leading cause of cancer-related deaths in the world. Overall, 80%–85% of lung cancer cases are nonsmall-cell lung cancer (NSCLC), and the subtypes of NSCLC mainly include lung adenocarcinoma (LUAD) and lung squamous cell carcinoma (LUSC) [1]. In the past 20 years, LUAD which accounts for approximately 40% of cases has become the most common subtype of NSCLC in most countries [2]. At present, most cases of LUAD are at an advanced stage when they are discovered [3]. Regular imaging examinations can increase the detection rate of LUAD in the curable stage, which greatly reduces lung cancer-related deaths, and avoids expensive treatment in the later period [4]. The latest World Health Organization (WHO) classification posits that LUAD tumors de-

velop in a typical sequence: atypical adenomatous hyperplasia (AAH) to adenocarcinoma *in situ* (AIS) to minimally invasive adenocarcinoma (MIA) to invasive adenocarcinoma [5]. Driver gene mutations in LUAD can be divided into three categories: EGFR mutations and ALK rearrangements; ROS1 rearrangements, RET rearrangements, and MET exon 14 deletion; and PIK3CA and other gene mutations [6].

In the process of cancer cell mitosis, the number of chromosomes of offspring cells often changes; that is, the cells become aneuploid. The unequal segregation of chromosomes is an important cause of aneuploidy [7]. Centromeric protein M (CENPM) is an important member of the constitutive centromeric-associated network (CCAN) protein family [8]. It is located on the inner kinetochore, and its function is to ensure the correct formation of centromeres

and kinetochores. CENPM also plays an important role in the normal division of cells. When the expression of CENPM is abnormal, it can bind to other centromeric proteins to form an important complex, which may lead to chromosome instability, thereby inducing gene mutations and causing tumors [9]. In addition, it has been reported that high CENPM expression is associated with primary hepatocellular carcinoma, bladder cancer, melanoma, and head and neck squamous cell carcinoma, suggesting that CENPM can be used as a new biomarker of tumor prognosis [10]. However, whether CENPM can act as an oncogene by interfering with the cell cycle process remains unknown.

In the current study, we found that the expression of CENPM mRNA is upregulated in LUAD. LUAD patients with high CENPM expression showed a low survival rate, which suggested a poor clinical outcome. Bioinformatics analysis and related experiments verified that CENPM promotes LUAD progression and accelerates the cell cycle of LUAD cells by activating the mTOR pathway. Thus, CENPM may control LUAD progression.

Materials and Methods

Bioinformatics analysis of CENPM

Six GEO LUAD chip datasets (GSE116959, GSE43458, GSE40419, GSE19804, GSE10072, and GSE118370) and the TCGA-LUAD RNA-seq dataset were used to analyze the expression of CENPM in LUAD tissues and normal lung tissues. All LUAD chip data differential analyses were performed with the limma package of the R language (version 3.42.2), and TCGA-LUAD data differential analysis was completed with the DEseq2 package (version 1.26.0). RNA-seq data from 33 normal tissue samples and 115 tumor tissue samples were used to further verify the expression of CENPM, and a box plot of the differences was generated according to the results of validation analysis. Then, the correlation between CENPM expression and the clinicopathological characteristics and survival prognosis of patients with LUAD was analyzed using the TCGA dataset online analysis tools LinkedOmics (<http://www.linkedomics.org/>) and KM plotter (<https://kmplot.com/analysis/>).

Cell culture

The Beas-2B, A549, 95D, PC-9, and NCI-H1975 cell lines were purchased from ATCC (Manassas, USA). DMEM (Procell, Wuhan, China) supplemented with 10% fetal bovine serum (FBS; WISENT, Nanjing, China) and 1% penicillin/streptomycin was used to culture the Beas-2B, A549 and PC-9 cell lines. The 95D and NCI-H1975 cell lines were cultured in RPMI 1640 medium (Procell) supplemented with 10% FBS and 1% penicillin/streptomycin. Cells were incubated in a standard incubator with 5% CO₂ at 37°C.

qRT-PCR

Total RNA was isolated from cells using the RNeasy spin kit (Qiagen, Beijing, China) according to the manufacturer's instructions. The purity and concentration of RNA were examined by a nucleic acid protein detector (Thermo Scientific, Waltham, USA). RNA samples were reverse transcribed using a RevertAid First Strand kit (Thermo Scientific). qRT-PCR was performed with a 7500 Fast Real-Time PCR System using SYBR Green Master (ROX) reagent (Roche, Basel, Switzerland). The sequences of the primers were as follows: CENPM forward 5'-CAGTCTCCAGAACACA GAGGAGTC-3' and reverse 5'-CACCTGTGGCGAGGAAAC-3'; GAPDH forward 5'-ACAGCCTCAAGATCATCAGC-3' and reverse 5'-

GGTCATGAGTCCCTCCACGAT-3'. The data were analyzed using the 2^{-ΔΔCT} method. GAPDH expression was used for the normalization of CENPM expression level.

Cell transfection

The lentiviral construct that expresses CENPM was pLVX-puro-CENPM (Oorui Bio, Changsha, China). Human CENPM was prepared by qRT-PCR. CENPM cDNA sequence was subcloned into the vector. Cells without any treatment were used as the blank group; cells transfected with negative sequence served as the normal control (NC) group; cells transfected with pLVX-puro-CENPM served as the CENPM-OE group; cells transfected with pLVX-puro (Oorui Bio) served as the vector group. To knock down CENPM, two short hairpin RNA (shRNA) sequences (shCENPM-1 and shCENPM-2) were designed by the BLOCK-iT™ RNAi Designer (<https://rnaidesigner.thermofisher.com/rnaidesigner/>). The shRNA sequences targeting CENPM2 were as follows: shCENPM-1 sense 5'-GATCCGCTTCGTGCTGACTCCATAAACTCGAGTTTATGGAGTCA GCACGAAGCTTTTTG-3' and antisense 5'-AATTCAAAAAGCTTCG TGCTGACTCCATAAACTCGAGTTTATGGAGTCAGCACGAAGCG-3'; shCENPM-2 sense 5'-GATCCGCGTGTACATCTCCATTTAAC TCGAGTTAAATGGAGATGTAACACGCTTTTTG-3' and antisense 5'-AATTCAAAAAGCGTGTACATCTCCATTTAACTCGAGTTAAAT GGAGATGTAACACGCG-3'. shRNA sequences were inserted into the pLKO.1 (Tiangen Biotech) cloning vector using the pLKO.1-based lentiviral shRNA technique. sh-NC (10879) was obtained from Addgene (Watertown, USA).

The above plasmids for CENPM overexpression or knockdown were cotransfected with pMD2.G and psPAX2 (Fenghui Bio, Changsha, China) into 293T cells (Thermo Scientific), and recombined lentiviral vectors were collected 48 h after transfection and used to infect cells. After infection for 48 h, 1.5 µg/mL puromycin was used continuously to screen and expand the cells. Stably-expressed cells were selected for subsequent experiments.

Cell proliferation assay

Cell proliferation was measured using Cell Counting Kit-8 (CCK-8; Dojindo, Tokyo, Japan). A total of 2 × 10³ cells were suspended in 100 µL of cell culture medium, seeded to a 96-well plate, and cultured in the incubator with 5% CO₂ at 37°C. After the culture was completed, the cells were incubated with 10 µL of CCK8 solution and incubated for another 2 h. Then the absorbance of each well at 450 nm was detected with a microplate reader (Epoch, Tokyo, Japan).

Cell invasion and migration assays

Transwell chambers (Corning Co., Corning, USA) and 24-well Transwell inserts (8 µm in aperture; BD Biosciences) were used for cell migration and invasion assays. For the migration assay, 5 × 10⁴ cells were placed into the upper chambers. For the invasion assay, 1 × 10⁵ cells were seeded into the upper chambers coated with Matrigel (Corning Co.). DMEM supplemented with 5% FBS was added to the lower chambers. These 24-well Transwell plates were cultured in the incubator (with 5% CO₂ at 37°C) for 6 h (migration) or 24 h (invasion). Then, the cells were fixed by 4% formaldehyde for 30 min, and then subject to crystal violet (Beyotime, Shanghai, China) staining for 20 min. Three fields of view were randomly selected under a CKX41 microscope (Olympus, Tokyo, Japan) to

take pictures, and the number of cells passed the membrane was counted.

Wound healing assay

Cell migration ability was analyzed by wound healing assay. After lentivirus or drug treatment for 48 h, cells were plated in 6-well plates at about 5×10^5 cells/well and allowed to grow to confluence. The wound was scratched using a tip and washed with serum-free medium to remove detached cells. Then the cells were cultured in complete medium. Wound healing process was monitored under a microscope (Leica, Wetzlar, Germany) and photographed at 0 h, 24 h and 48 h later.

Cell cycle assay

When transfected cells reached approximately 70%–80% confluence, they were digested with trypsin and counted. A total of 1×10^5 cells were seeded into a 10-cm dish. After 48 h of culture, the cells were digested and collected, and then fixed with 75% ethanol overnight at 4°C. After treatment with RNase A (Sigma-Aldrich), cells were stained with PI (Dojindo) for 20 min at room temperature in the dark. Flow cytometry was performed to analyze the cell distribution in each phase within 24 h.

Cell apoptosis assay

After cell lentivirus or drug treatment, CENPM-knockdown A549 and PC-9 cells or CENPM-overexpressing NCI-H1975 and 95-D cells were digested and harvested for apoptosis analysis. The Annexin V-FITC/PI detection kit (Beibo Biological, Shanghai, China) was used for the determination of cell apoptosis according to the manufacturer's instructions. Apoptosis was detected by flow cytometry.

Flow cytometric analysis

The cells were collected in a 15 mL of centrifuge tube and washed with $1 \times$ binding buffer. Centrifugation was used to remove the washing liquid. Suspension cells were suspended with 200 μ L of $1 \times$ binding buffer and 5 μ L of Annexin V. The mixture of 200 μ L of $1 \times$ binding buffer and 5 μ L of PI was added to each tube at room temperature and incubated in the dark for 15 min. Totally 20,000 events were collected in each sample. Data analysis was performed using a BD AccuriR C6 (BD Biosciences, Franklin Lakes, USA).

Western blot analysis

Protein concentration was determined using a Pierce BCA Protein Assay Kit (Thermo Scientific). After separation by 10% SDS-PAGE, the proteins were transferred onto polyvinylidene difluoride membranes. Then, the membranes were blocked with TBST containing 5% nonfat skimmed milk and incubated with primary antibodies, including GAPDH rabbit pAb and GAPDH mouse pAb (Proteintech, Wuhan, China). Subsequently, the membranes were incubated with the corresponding HRP-conjugated secondary antibodies (Cell Signaling Technology, Boston, USA). Signal detection was conducted with an enhanced chemiluminescence (ECL) system (Tanon, Shanghai, China). GAPDH was used as a loading control.

In vivo xenograft study

Nude mice aged 5–6 weeks (Hunan SJA, Changsha, China) were randomly divided into two groups in two cages, with 6 mice in each group. The two groups of mice were subcutaneously injected with A549 + LV-shCENPM-1 and NC A549 + LV-shNC cells into the axilla

after acclimatization to the environment for 7 days. The amount of injected cells was 1×10^7 cells/mouse. Seven days after the subcutaneous injection of tumor cells, the tumors became visible to the naked eye, and the size of the subcutaneously transplanted tumors was measured every 5 days. On the 32nd day, the nude mice were sacrificed, and tumors were collected and photographed for statistical analysis, and saved for subsequent tests.

Immunohistochemical staining

The tissue sections were deparaffinized and then placed in antigen retrieval solution for repair, and then incubated with 100 μ L of the diluted primary antibody (MCM2, 1:50; PCNA, 1:500; E-cad, 1:1000; Vimentin, 1:5000) overnight at 4°C. Then 1 secondary antibody solution (1:50) was added and incubated at room temperature for 20 min. Horseradish peroxidase-labeled streptavidin was incubated with the tissues for further 20 min at room temperature. After washing with PBS, DAB was added for staining and then the tissues were observed under a microscope until they appear light yellow. ddH₂O was used to stop the reaction. The tissues were further stained with hematoxylin, and then observed with the microscope.

Statistical analysis

GraphPad Prism 7.0 software was used to prepare the graphs, and SPSS 17.0 statistical software was used to analyze the experimental results. Comparisons between the two groups were performed with the unpaired *t* test, and comparisons between multiple groups were performed with one-way ANOVA and Dunnett's multiple comparisons test. *P* < 0.05 was considered statistically significant.

Results

CENPM upregulation indicates poor outcome of LUAD patients

We investigated the expression level of CENPM in LUAD patients using six GEO LUAD chip datasets (GSE116959, GSE43458, GSE40419, GSE19804, GSE10072, and GSE118370) and the TCGA-LUAD dataset. The results showed that the expression level of CENPM was significantly upregulated in LUAD tumors compared with that in the lung tissues of healthy populations (Tables 1 and 2, and Figure 1A,B). In addition, RNA-seq data from 33 normal tissue samples and 115 tumor tissue samples further verified that the expression level of CENPM is higher in LUAD than in normal tissues (Figure 1C). KM plotter analysis revealed that CENPM is significantly related to the overall survival of patients with LUAD (*n* = 719) (Figure 1D). Patients with high expression of CENPM showed poor clinical outcomes (hazard ratio > 1, *P* < 0.01). Moreover, in the data of 513 cases of LUAD from a pancancer dataset, the overall survival was found to be shortened in LUAD patients with high expression level of CENPM (Figure 1E). Thus, high CENPM expression may be a significant risk factor for patients with LUAD.

Experimental cell selection and infection efficiency detection

According to our analysis of the mRNA and protein expression levels of CENPM in LUAD cells (Figure 2A,B), the LUAD cell lines A549 and PC-9, which have relatively high expression levels of CENPM, were selected to construct CENPM-knockdown cell lines, and the relative expression levels were detected. The LUAD cell lines with lower CENPM expression, NCI-H1975 and 95-D, were used to construct CENPM-overexpressing cell lines. Lentiviruses

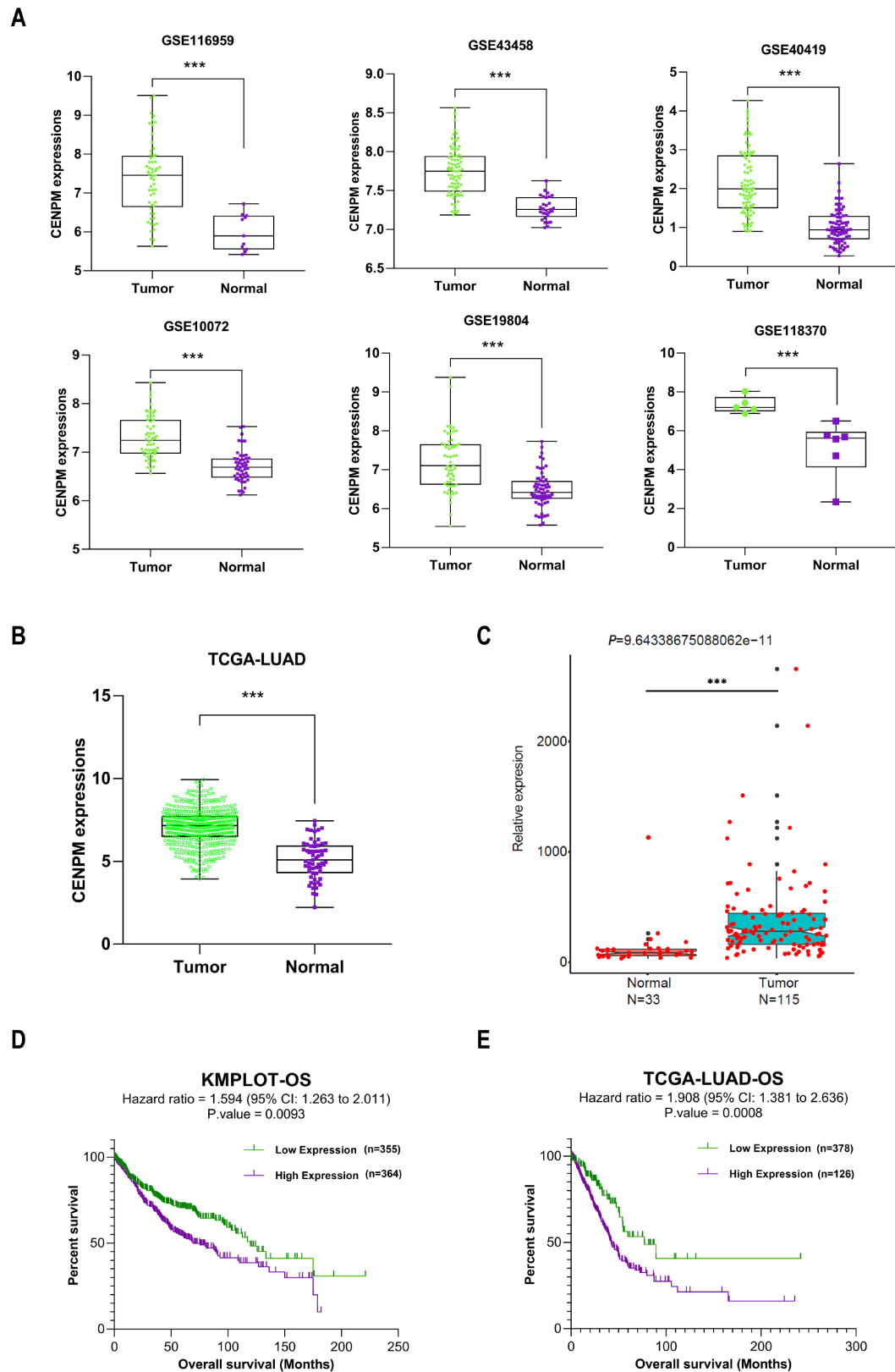


Figure 1. CENPM upregulation is related to the prognosis of LUAD patients (A) Box plot of CENPM expression in 6 LUAD chip datasets. (B) Box plot of CENPM expression in the TCGA-LUAD RNA-seq dataset. (C) Box plot of CENPM expression in the XWFA RNA-seq dataset. (D) KM plotter analysis of the correlation between the expression level of CENPM and the overall survival of patients with LUAD. (E) Correlation between the expression level of CENPM and the overall survival of patients with LUAD in the TCGA-LUAD dataset.

Table 1. Differential expression of CENPM in six LUAD chip datasets

Dataset	logFC	Average expression	<i>t</i>	<i>P</i>	Adjusted <i>P</i>	<i>B</i>	Gene	Change
GSE118370	2.388628	6.292234	4.072177	0.001414	0.040279	-0.966	CENPM	UP
GSE40419	1.133927	1.619896	10.628410	2.29E-20	3.77E-19	35.571	CENPM	UP
GSE116959	1.397360	7.165771	4.765209	1.01E-05	0.000165	3.046	CENPM	UP
GSE43458	0.475103	7.613987	7.988550	1.40E-12	3.66E-11	18.099	CENPM	UP
GSE19804	0.689767	6.835489	6.363994	3.71E-09	3.34E-08	10.330	CENPM	UP
GSE10072	0.586334	7.027097	7.844583	3.26E-12	4.09E-11	17.069	CENPM	UP

Table 2. Differential expression of CENPM in the TCGA-LUAD RNA-seq dataset

Dataset	logFC	Average expression	<i>t</i>	<i>P</i>	Adjusted <i>P</i>	<i>B</i>	Gene	Change
TCGA-LUAD	1.971579	6.884412	13.19161	6.66E-35	1.31E-33	68.336	CENPM	UP

carrying shNC, shCENPM-1 and shCENPM-2 plasmids were used to infect A549 and PC-9 cells, and the knockdown efficiency was verified by qPCR and western blot analysis (Figure 2C,D). The results showed that compared with the NC group, the shCENPM-1 and shCENPM-2 groups had significantly reduced mRNA and protein expression of CENPM ($P < 0.01$), and the knockdown efficiency of shCENPM-1 was stronger than that of shCENPM-2, proving successful CENPM knockdown in A549 and PC-9 cells. Similarly, lentiviruses carrying pLVX-puro and pLVX-puro-CENPM plasmids were used to infect NCI-H1975 and 95-D cells to generate the vector and CENPM-OE groups. Additionally, qPCR and western blot analysis were used to determine the overexpression efficiency. As shown in Figure 2E,F, NCI-H1975 and 95-D cells in the CENPM-OE group showed significantly upregulated expression of CENPM protein and mRNA ($P < 0.01$). Thus, CENPM overexpression cell lines were also successfully constructed.

CENPM promotes the proliferation of LUAD cells

CCK-8 cell proliferation assay was used to detect the effects of knockdown and overexpression of CENPM on the proliferation of LUAD cells. The results showed that the proliferation ability of A549 and PC-9 cells in the shCENPM-1 and shCENPM-2 groups was lower than that of the cells in the shNC group. Cell proliferation was significantly inhibited, and the result was more obvious at 72 h ($P < 0.01$; Figure 3A,B). Similarly, the results of the CENPM overexpression experiments in cell lines were also in line with expectations. Stable overexpression of CENPM promoted the proliferation of NCI-H1975 and 95-D cells *in vitro*, and the results at 72 h were more significantly different ($P < 0.01$; Figure 3C,D). In summary, CENPM overexpression can promote the proliferation of LUAD cells, and knockdown of CENPM can inhibit the proliferation of LUAD cells.

CENPM promotes G1/S transition and DNA synthesis of LUAD cells

We used PI staining solution to stain LUAD cells and further used flow cytometry to detect the effects of knockdown and overexpression of CENPM on the cell cycle distribution of LUAD cells. As shown in Figure 4A,B, after knockdown of CENPM in A549 and PC-9 cells, the cells showed obvious changes in cell cycle distribution. Compared with cells in the shNC group, A549 and PC-9 cells in the shCENPM-1 and shCENPM-2 groups showed more cells in the G1 phase ($P < 0.01$); that is, a "G1 phase block" occurred. Conversely, overexpression of CENPM promoted G1/S transition in

NCI-H1975 and 95-D cells. Compared with that in the control group, the percentage of S phase cells in the CENPM-OE group was significantly increased, while the percentage of G1 phase cells was decreased ($P < 0.01$); that is, the proportion of cells in the DNA replication phase was increased (Figure 4C,D). In summary, CENPM may promote the proliferation of LUAD cells by promoting cell cycle G1/S transition and DNA synthesis.

CENPM inhibits the apoptosis of LUAD cells

To study the potential role of CENPM in regulating the apoptosis of LUAD cells, we used Annexin V/PI staining and flow cytometry analysis to detect the effects of knockdown and overexpression of CENPM on the apoptosis of LUAD cells. The results showed that the number of apoptotic A549 and PC-9 cells in the shCENPM-1 and shCENPM-2 groups was significantly higher than that in the shNC group (Figure 5A,B). In contrast, the number of apoptotic NCI-H1975 and 95-D cells in the CENPM-OE group was significantly lower than that in the vector group (Figure 5C,D). All the results were significantly different, indicating that CENPM can inhibit the apoptosis of LUAD cells.

CENPM promotes the migration and invasion of LUAD cells

Transwell cell migration and invasion experiments confirmed the effects of knockdown or overexpression of CENPM on the migration and invasion of LUAD cells. The results showed that in A549 and PC-9 cells in the shCENPM-1 and shCENPM-2 groups, the number of cells that migrated through the chamber and the number of invaded cells were significantly lower than those in the shNC group (Figure 6A,B,E,F), while in H1975 and 95-D cells in the CENPM-OE group, the number of cells passed through the chamber and the number of invaded cells were significantly higher than those in the vector group (Figure 6C,D,G,H). The above results were significantly different, further confirming that CENPM can promote the migration and invasion of LUAD cells.

CENPM promotes tumor growth *in vivo*

The effect of CENPM on tumor growth was analyzed *in vivo*. Figure 7A shows the transplanted tumors in the A549 + LV-shNC group and A549 + lv-shCENPM-1 group. As shown in Figure 7B, compared with that in the nude mice in the A549 + LV-shNC group, the growth of transplanted tumors in the nude mice in the A549 + LV-shCENPM-1 group was significantly inhibited. The volume difference of transplanted tumors between the two groups increased

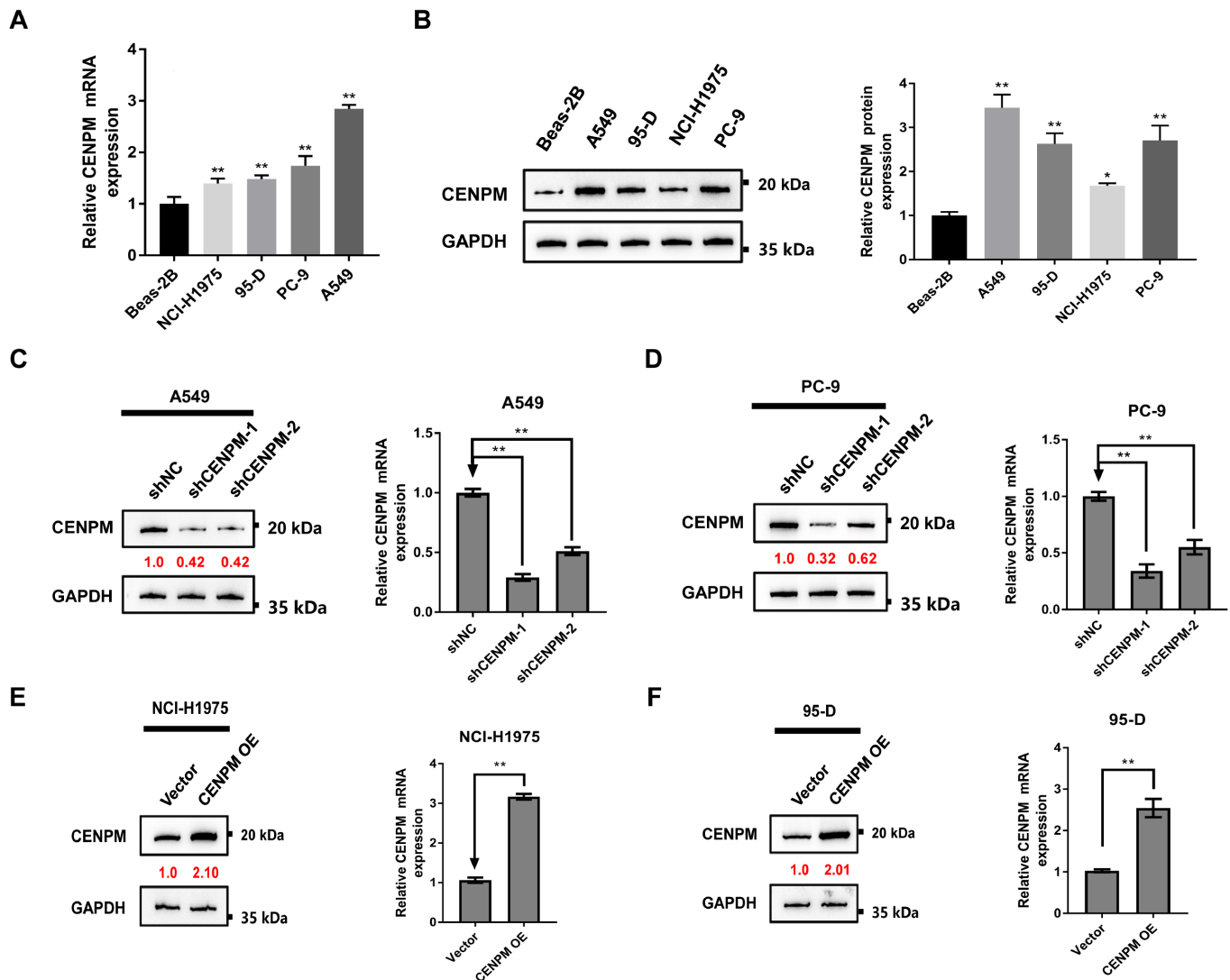


Figure 2. CENPM knockdown and overexpression in LUAD cells (A) Detection of CENPM mRNA expression in Beas-2B alveolar epithelial cells and four LUAD cell lines. (B) Detection and quantification of CENPM protein expression in Beas-2B alveolar epithelial cells and four LUAD cell lines. (C) Detection of mRNA and protein expression after knockdown of CENPM in A549 cells with two shRNAs. (D) Detection of mRNA and protein expression after knockdown of CENPM in PC-9 cells using two shRNAs. (E) Detection of mRNA and protein expression after overexpression of CENPM in H1975 cells. (F) Detection of mRNA and protein expression after overexpression of CENPM in 95-D cells. All data are the results of three independent experiments.

significantly with the extension of the inoculation time, and the difference between the two groups was statistically significant ($P < 0.01$). The proliferation of transplanted tumors was decreased significantly after knockdown of CENPM, which proved that CENPM can promote tumor growth *in vivo*.

We compared the protein expressions of MCM2 and PCNA between the A549 + LV-shCENPM-1 group and the A549 + LV-shNC group by western blot analysis. The results showed that the expressions of both proteins were decreased significantly after knockdown of CENPM, which proved that CENPM can promote the proliferation of LUAD cells *in vivo*, and the changes in MCM2 and PCNA may be related to the proliferation effects of CENPM (Figure 8A–F). As shown in Figure 8E, knockdown of CENPM protein significantly increased the level of E-cad in transplanted tumors, increased the adhesion between cells, and decreased the metastasis and invasion ability of LUAD cells. In contrast, the vimentin protein level in the A549 + LV-

shCENPM-1 group was significantly lower than that in the A549 + LV-shNC group (Figure 8F), indicating a decrease in epithelial and mesenchymal changes. The results also indicated that the metastasis and invasion ability of the transplanted tumor cells was decreased after CENPM knockdown. Furthermore, we also used transplanted tumor sections from two groups of nude mice for immunohistochemical staining. As shown in Figure 8G, the immunohistochemistry results are consistent with the protein detection results.

CENPM down-regulates the activity of mTOR protein *in vivo*

We used the expression data matrix of 517 tumors from the TCGA-LUAD dataset to establish a gene network related to CENPM expression based on the R language in an attempt to analyze the functions of genes related to CENPM. We found that CENPM-related genes were significantly involved in mTORC1 regulation and the

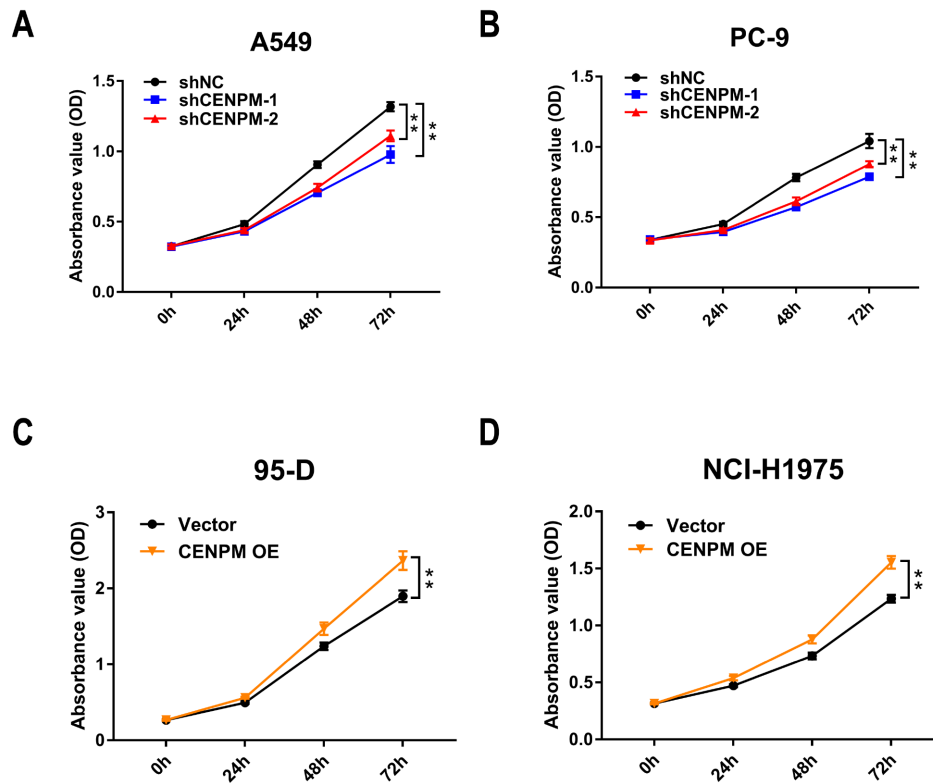


Figure 3. CENPM affects the proliferation of LUAD cells (A) Two shRNAs were used to knock down CENPM in A549 cells, and a CCK8 kit was used to detect cell proliferation within 72 h. (B) Two shRNAs were used to knock down CENPM in PC-9 cells, and a CCK8 kit was used to detect the proliferation of each group of NCI-H1975 cells after 72 h. (C) After induction of overexpression of CENPM in NCI-H1975 cells, a CCK8 kit was used to detect cell proliferation within 72 h. (D) A CCK-8 kit was used after induction of overexpression of CENPM in 95-D cells to detect cell proliferation within 72 h. All data are the results of three independent experiments.

PI3K/AKT/mTOR signaling pathway (Figure 9A,B).

To further verify whether the PI3K/AKT/mTOR signaling pathway is involved in the CENPM-based regulation of the biological function of LUAD cells, we used western blot analysis to assess tumor tissues from nude mice transplanted with A549 + LV-shNC or A549 + LV-shCENPM-1 cells. The levels of mTOR protein and phosphorylated mTOR protein (p-mTOR) were assessed. The western blot analysis results showed that compared with the respective levels in the A549 + LV-shNC group, the level of mTOR protein was not significantly different after CENPM knockdown, but the level of p-mTOR was significantly downregulated (Figure 9C), suggesting that CENPM does not affect mTOR protein expression but affect its kinase activity, which further regulates the biological function of LUAD cells by regulating the phosphorylation of the mTOR protein. This may be a potential biological mechanism supporting the development of CENPM as an oncogene in LUAD.

CENPM regulates PI3K/AKT/mTOR pathway by affecting mTOR phosphorylation

To further clarify whether CENPM affects the mTOR signaling pathway and whether it regulates the biological functions of LUAD cells through the mTOR signaling pathway, we carried out a series of *in vitro* experiments. We stably knocked down CENPM in A549 and PC-9 LUAD cell lines and then analyzed the levels of p-mTOR and mTOR in the cell lines by western blot analysis. We found that knocking down CENPM significantly decreased the level of p-mTOR

(Supplementary Figure S1A,B). In contrast, we used a lentiviral system to stably overexpress CENPM in NCI-H1975 and 95-D LUAD cell lines with otherwise low expression of CENPM, and found that overexpression of CENPM significantly upregulated the p-mTOR level (Supplementary Figure S1C,D), indicating that CENPM has a positive regulatory effect on the mTOR signaling pathway and can promote the activation of mTOR.

To further verify whether the mTOR signaling pathway is indeed a key pathway by which CENPM regulates the biological functions of LUAD cells, we used the mTOR inhibitor DIM-C-pPhOH (20 μ M) to inhibit the phosphorylation of mTOR (Supplementary Figure S2A). In the NCI-H1975 cell line, after stably overexpressing CENPM and treatment with the mTOR inhibitor DIM-C-pPhOH to inhibit the mTOR pathway, the proliferation effect of CENPM on cells was partially blocked (Supplementary Figure S2B), which promoted the cell cycle. G1/S phase transformation was partially blocked, G1 phase blockade occurred (Supplementary Figure S3A, B), the number of apoptotic cells increased, cell migration and healing were significantly reduced (Figure 10A), and the number of migrating cells was decreased significantly (Figure 10B-E). These results revealed that CENPM possibly functions as an oncogene by activating the PI3K/AKT/mTOR pathway in LUAD cells.

Discussion

Through clinicopathological characteristics and survival-related prognostic analysis, we found that the expression level of CENPM is

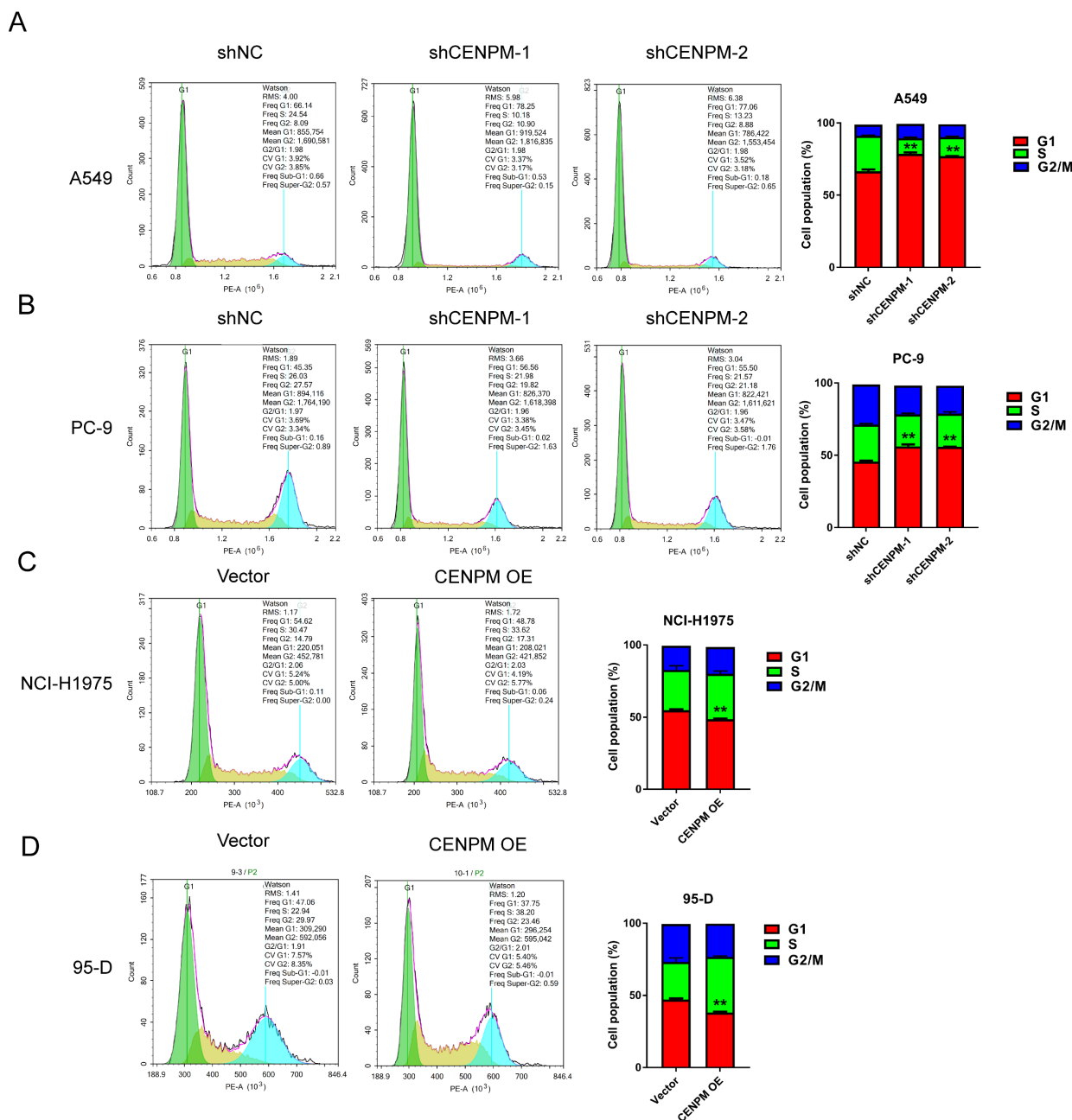


Figure 4. The effect of CENPM on the cell cycle of LUAD cells (A) Two shRNAs were used to knock down CENPM in A549 cells, and PI staining and flow cytometry were used to detect the cell cycle distributions. (B) Two shRNAs were used to knock down CENPM in PC-9 cells, and PI staining and flow cytometry were used to detect the cell cycle distributions. (C) PI staining and flow cytometry were used to detect the cell cycle distributions after induction of overexpression of CENPM in NCI-H1975 cells. (D) PI staining and flow cytometry were performed after induction of overexpression of CENPM in 95-D cells, and a flow cytometer was used to detect cell cycle distributions. All data are the results of three independent experiments.

significantly related to the clinical TNM stage and class in LUAD, and a high expression level of CENPM is a very significant risk factor for the prognosis of patients with LUAD. CENPM is abnormally highly expressed in LUAD and is significantly correlated with the clinicopathological characteristics and survival-related prognosis of patients, suggesting that CENPM may play a role in promoting LUAD and may be related to tumor cell proliferation and disease progression. To verify these results, we used experiments to prove that CENPM affects the biological functions of LUAD cells.

CENPM can not only maintain the stability and integrity of the centromere structure but also participate in the regulation of cell division and proliferation [11]. Overexpression of CENPM induces uneven chromosome separation in cells during mitosis, which may lead to an unequal number of chromosomes allocated to progeny cells, resulting in loss or gain of entire chromosomes in progeny cells [12]. After several cell cycles, aneuploid cells can carry one or more visible aberrations [13]; this kind of cell is more prone to chromosomal aberrations than normal cells [14]. Such cells also

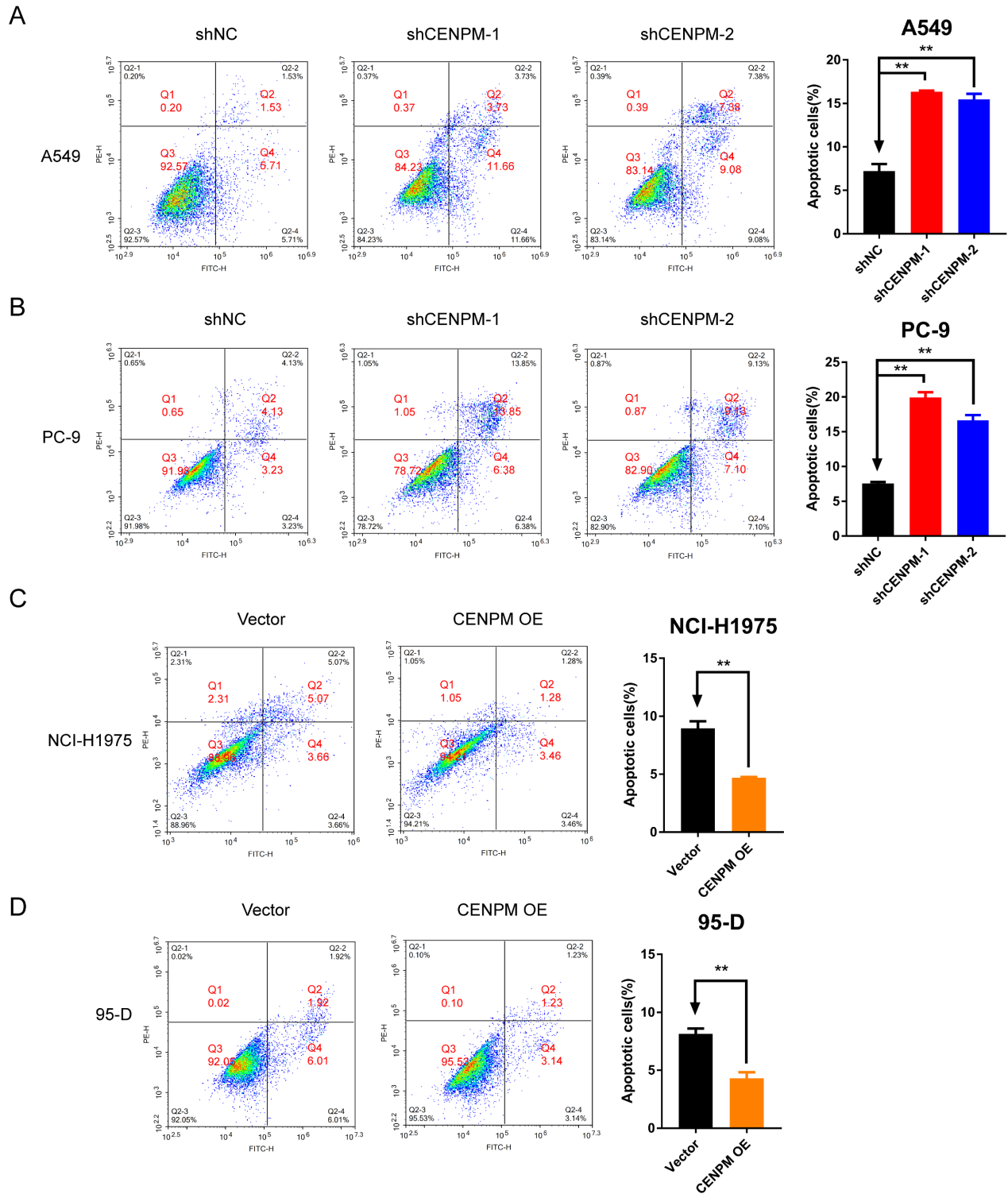


Figure 5. The effect of CENPM on the apoptosis of LUAD cells (A) Two shRNAs were used to knock down CENPM in A549 cells, and FITC/PI staining and flow cytometry were used to detect cell apoptosis. (B) Two shRNAs were used to knock down CENPM in PC-9 cells, and FITC/PI staining and flow cytometry were used to detect cell apoptosis. (C) After induction of overexpression of CENPM in NCI-H1975 cells, FITC/PI staining and flow cytometry were used to detect cell apoptosis. (D) After induction of overexpression of CENPM in 95-D cells, FITC/PI staining and flow cytometry were used to detect cell apoptosis. All data are the results of three independent experiments.

carry gene mutations and gene amplification because of many mechanisms that can damage the integrity of the genome and can

participate in regenerative cell death [15]. In contrast, when the expression of the CENPM gene is inhibited, the organization of

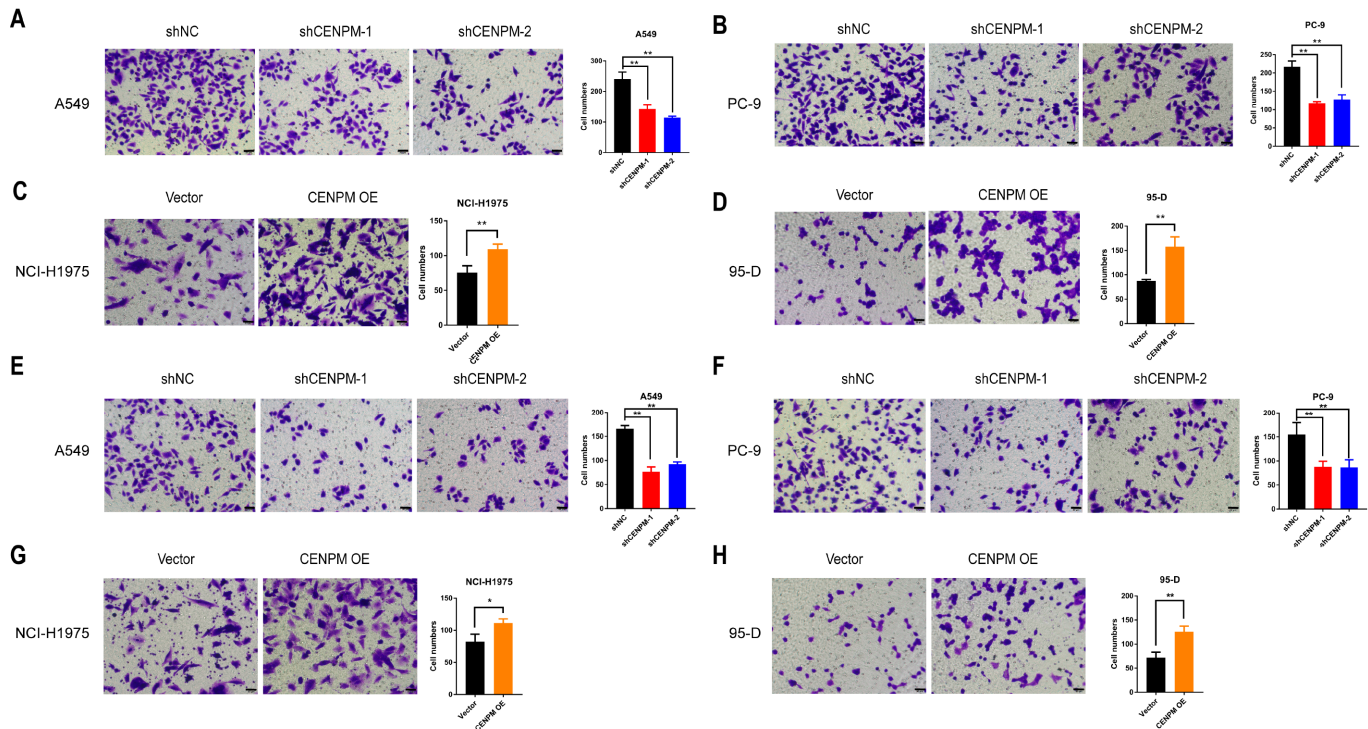


Figure 6. CENPM affects the migration and invasion abilities of LUAD cells (A) Two kinds of shRNAs were used to knock down CENPM in A549 cells, and the Transwell assay was used to detect cell migration ability. (B) Two kinds of shRNAs were used to knock down CENPM in PC-9 cells, and Transwell assay was used to test cell migration ability. (C) Transwell assay was used to detect cell migration ability after CENPM overexpression was induced in NCI-H1975 cells. (D) Transwell assay was used to detect cell migration ability after CENPM overexpression was induced in 95-D cells. All data are the result of three independent experiments. (E) Two shRNAs were used to knock down CENPM in A549 cells, and Transwell assay was used to detect cell invasion. (F) Two shRNAs were used to knock down CENPM in PC-9 cells, and Transwell assay was used to detect cell invasion. (G) NCI-H1975 cells were induced to overexpress CENPM, and Transwell assay was used to detect cell invasion ability. (H) After induction of overexpression of CENPM in 95-D cells, Transwell assay was used to detect cell invasion ability. All data are the results of three independent experiments.

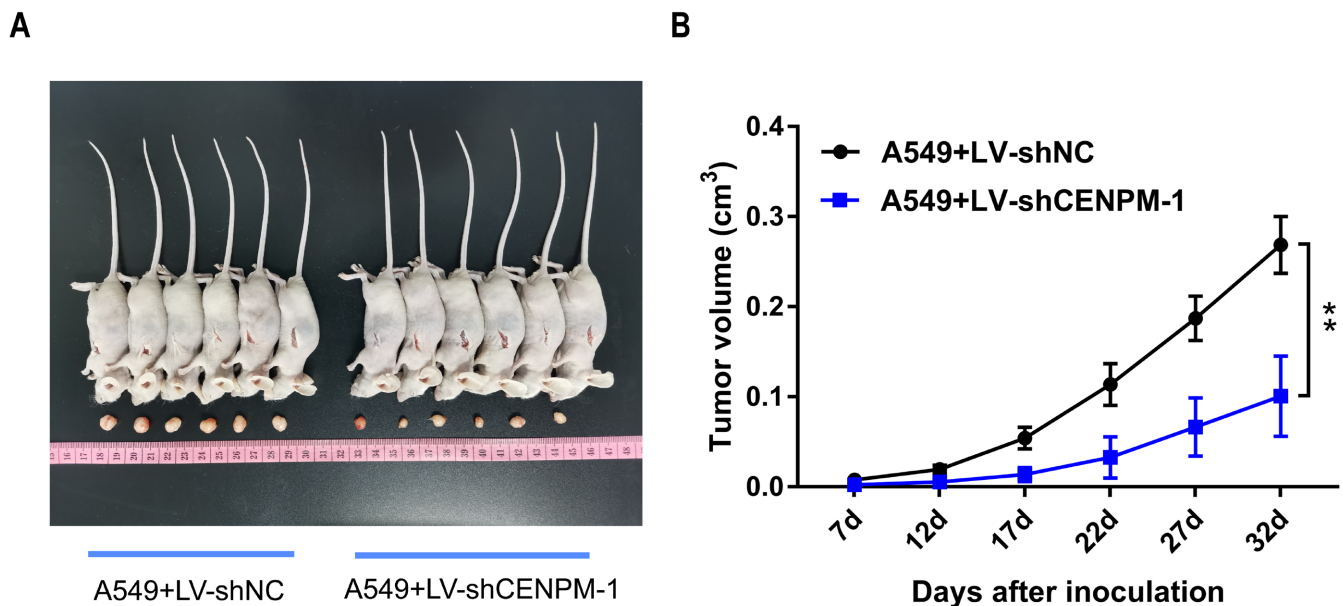


Figure 7. The effect of CENPM on tumor growth was detected by xenograft assay in nude mice (A) Tumors removed from the body of each group of nude mice after sacrifice. (B) Changes in the tumor volume of nude mice in each group during rearing.

chromosomes into chromatin and the formation of the centromere kinetochore complex (CKC) are defective, which hinders the pro-

cess of cell centromere assembly [16]. In turn, the chromosome doubling time is prolonged, and ultimately, the mitotic index of the

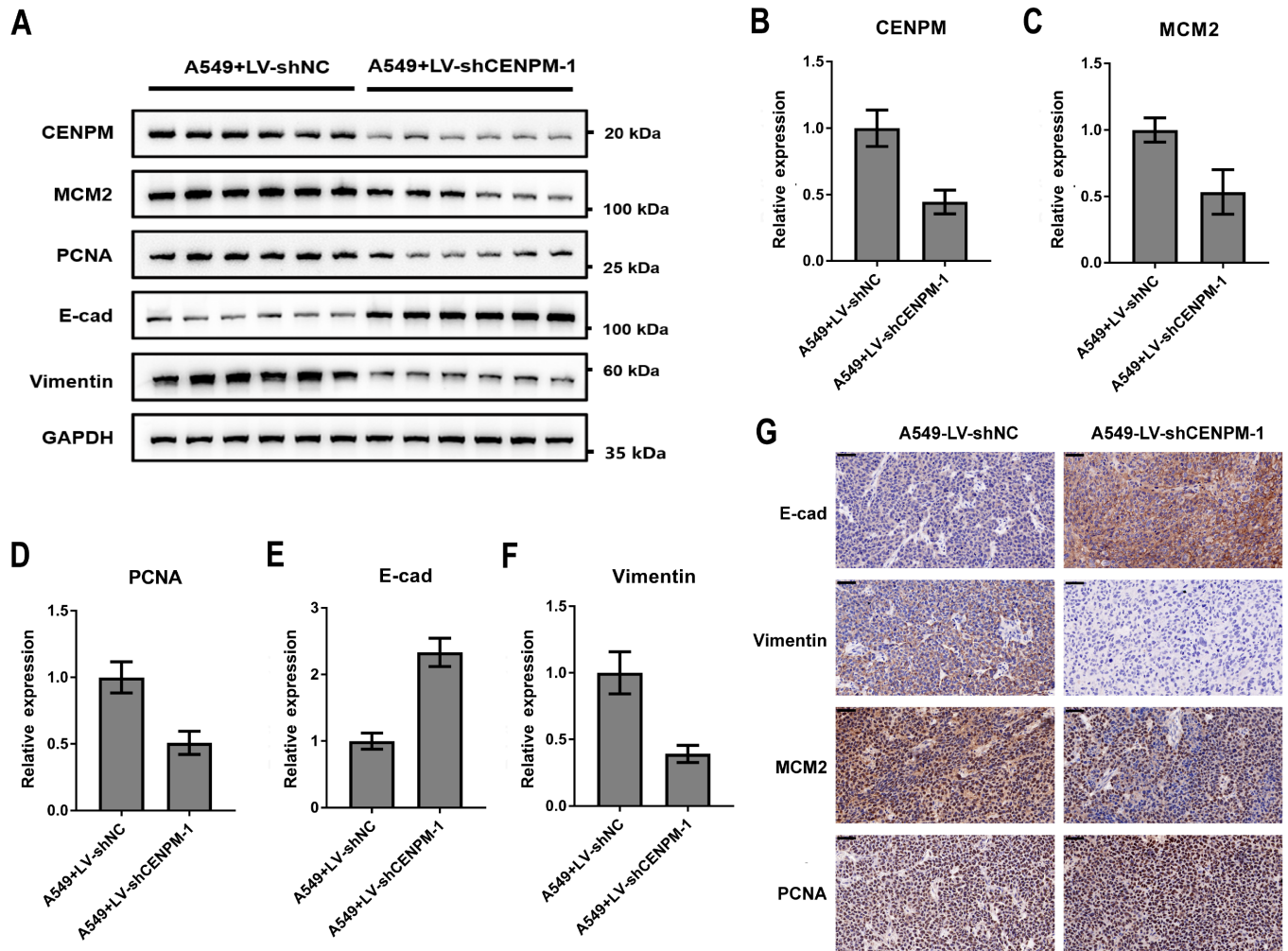


Figure 8. CENPM affects the expression of biochemical indicators in transplanted tumors (A) Western blot analysis of proteins in transplanted tumors. (B) Immunohistochemical analysis of the biochemical indicators in transplanted tumors. Scale bar: 50 μ m.

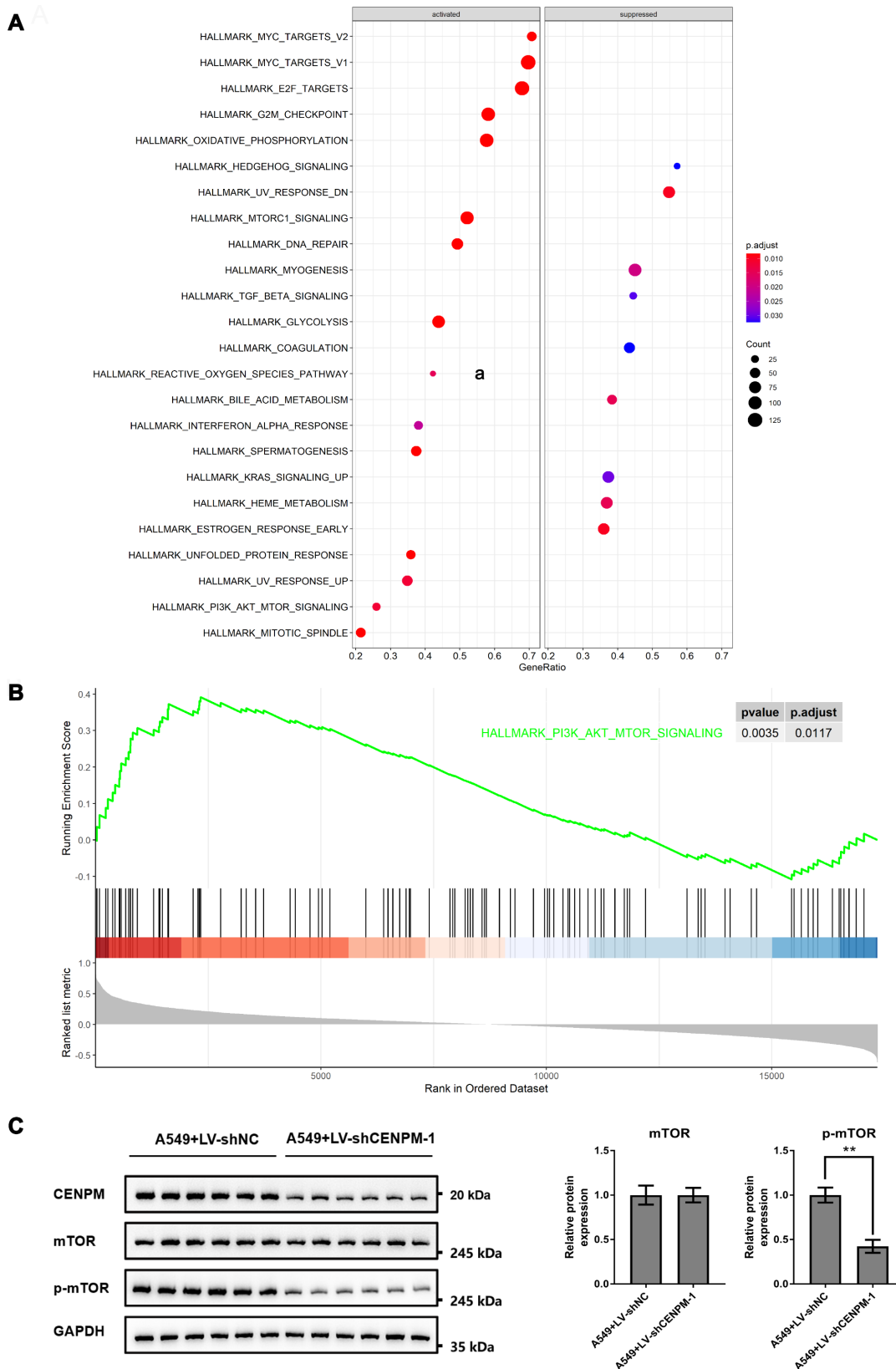
cell is greatly reduced [17]. These results show that CENPM plays an important role in tumor cell proliferation.

The PI3K/AKT/mTOR signaling pathway is a classic signaling pathway in tumor research. It has been proven to be abnormally activated in a variety of tumors [18]. Abnormal activation of this pathway can cause abnormal tumor transformation, promote tumor growth and metastasis, and affect tumor blood vessels [19]. In the clinical treatment of tumors, the activation of key factors in this pathway can also be used as an indicator to evaluate the prognosis of patients. Studies have shown that the expression of PI3K, AKT, and mTOR upregulated in non-small-cell lung cancer [20,21]. mTOR is a target protein downstream of AKT. mTOR is an atypical serine/threonine kinase and belongs to the phosphoinositide 3-kinase-related protein kinase (PIKK) family [22]. mTOR is the catalytic subunit of two protein kinase complexes: mTORC1 and mTORC2. The activation of mTORC1 is related to the regulation of mTOR proteins. The complex mTORC2 is different from mTORC1. It is not sensitive to rapamycin and participates in cell survival and proliferation. It is activated by AKT phosphorylation at serine 473, which controls the activity of AKT [23,24].

Previous studies have shown that CENPM is oncoprotein in LUAD. CENPM is highly expressed in LUAD cells and associated

with poor overall survival and increased rate of disease recurrence. Our results revealed that LUAD cells with low expression of CENPM had significantly inhibited proliferation, cell cycle arrest at the G1 phase and migration and invasion. In contrast, overexpression of CENPM promoted G1/S phase transition, increased DNA synthesis and promoted cell proliferation.

We also found that the expressions of MCM2, PCNA and vimentin in LUAD cells were decreased after CENPM was knocked down, and the expression of E-cad was increased, suggesting that the effect of CENPM on the proliferation, migration and invasion of LUAD cells may be a result of the effects on the above proteins. Bioinformatics analysis suggested that CENPM-related genes are significantly involved in the mTORC1 regulation and PI3K/AKT/mTOR signaling pathway. We also detected the expression of mTOR and p-mTOR in transplanted tumors in nude mice. The results proved that CENPM does not affect the expression of mTOR protein but does affect its kinase activity, which further regulates the biological functions of LUAD cells by regulating the phosphorylation of mTOR protein. Studies have shown that down-regulation of CENPM can inhibit the proliferation of pancreatic cancer cells through the mTOR/p70S6K signaling pathway, affect the cell cycle, and limit the migration and invasion of pancreatic



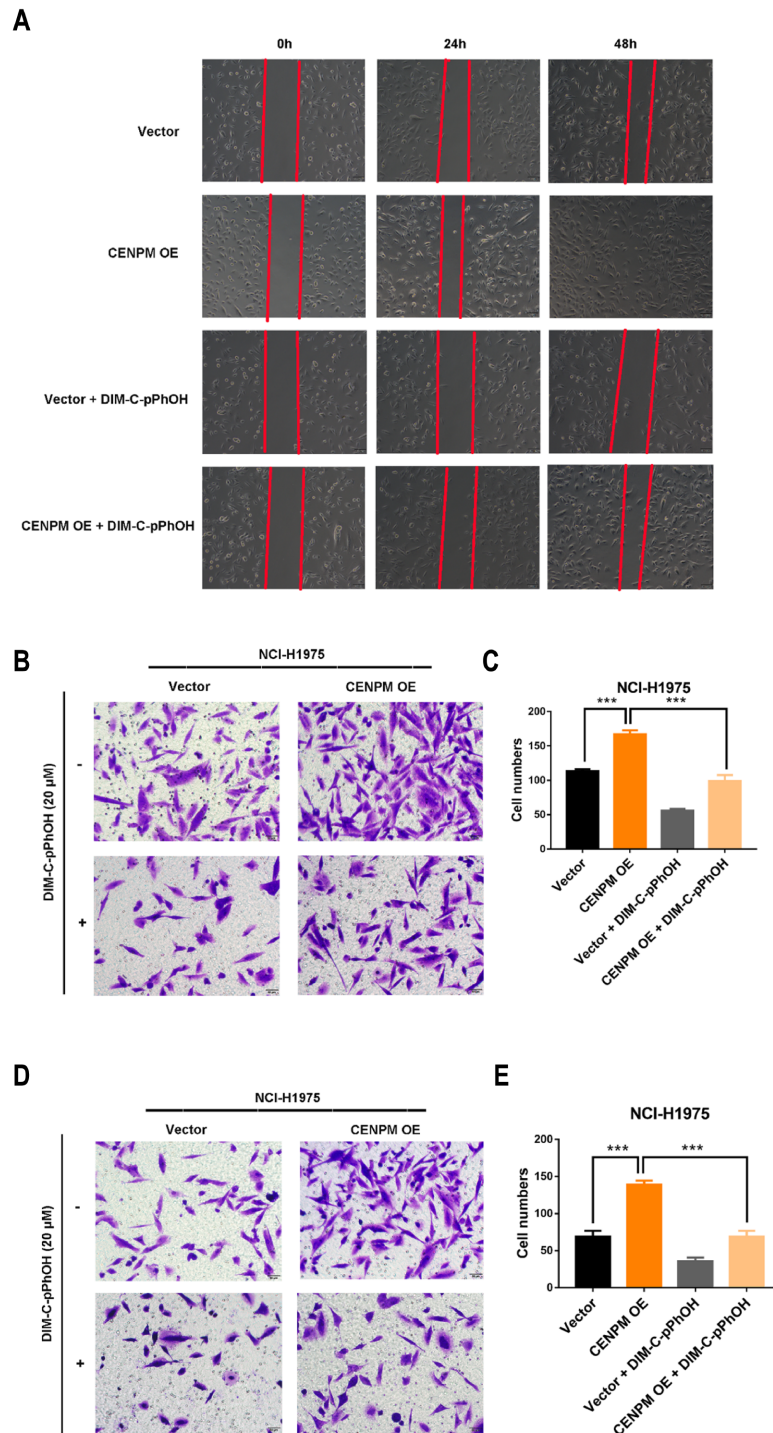


Figure 10. mTOR inhibition blocks the ability of CENPM on the migration and invasion of NCI-H1975 cells (A) Inhibition of mTOR partially blocked the ability of CENPM to promote cell migration. A lentiviral system was used to overexpress CENPM in NCI-H1975 cells. After treatment with DMSO or the mTOR inhibitor DIM-C-pPhOH (20 μ M) in control or CENPM-overexpressing cells for 48 h, wound healing assay was used to detect cell migration ability. Representative images of cell migration in each group are shown. (B) Inhibition of mTOR partially blocked the ability of CENPM to promote cell migration. CENPM was overexpressed in NCI-H1975 cells that were treated with DMSO or the mTOR inhibitor DIM-C-pPhOH (20 μ M) for 24 h. Transwell cell migration experiments were used to detect cell migration ability. Representative images of cell migration in each group are shown. (C) Quantitative statistics of the numbers of cells migrating through the chamber in each group. (D) Inhibition of mTOR partially blocked the ability of CENPM to promote cell invasion. CENPM was overexpressed in NCI-H1975 cells treated with DMSO or the mTOR inhibitor DIM-C-pPhOH (20 μ M) for 24 h. Transwell cell invasion assays were used to detect cell invasion ability. Representative graphs of cell invasion in each group are shown. (E) Quantitative statistics of the number of cells migrating through the chamber in each group. The data are the results of 3 independent repeated experiments. One-way analysis of variance was used to determine the *P* value. The data are shown as the mean \pm standard deviation of 3 independent repeated experiments.

cancer cells [25]. This finding is consistent with our bioinformatics analysis and the *in vivo* verification in nude mice. The interaction between CENPM and the PI3K/AKT/mTOR signaling pathway was preliminarily shown to be the key mechanism underlying the function of CENPM in LUAD. However, the specific regulatory details of CENPM are still unclear, and its molecular mechanism needs to be further explored.

In summary, our study showed that CENPM expression is increased in LUAD, particularly in patients with late-stage or metastatic disease, indicating that CENPM may serve as a biomarker to predict progression and metastasis. Our data also demonstrated that increased expression of CENPM plays a crucial role in the tumorigenesis of LUAD both *in vitro* and *in vivo* by modulating the PI3K/AKT/mTOR signaling pathway via the effects on mTOR phosphorylation.

Supplementary Data

Supplementary Data is available at *Acta Biochimica et Biophysica Sinica* online.

Funding

This work was supported by the grants from the National Natural Science Foundation, Regional Science Foundation Project (No. 81960322), Medical Reserve Personnel Training Program of Yunnan Provincial Health Commission (No. H-2018097), Joint Program of Applied Basic Research of Yunnan Provincial Department of Science and Technology-Kunming Medical University (No. 2018FE001(-247)), Medical Leading Talents Training Program of Yunnan Provincial Health Commission (No. L-2019028), the "Famous Doctor" Special Project of the Ten Thousand People Plan of Yunnan Province (No. C20096), and the Kunming Medical University Master's Innovation Fund (No. 2021S248).

Conflict of Interest

The authors declare that they have no conflict of interest.

References

- Zhang Y, Luo G, Etxeberria J, Hao Y. Global patterns and trends in lung cancer incidence: a population-based study. *J Thoracic Oncol* 2021, 16: 933–944
- Low JL, Huang Y, Sooi K, Ang Y, Chan ZY, Spencer K, Jayasekharan AD, *et al.* Low-dose pembrolizumab in the treatment of advanced non-small cell lung cancer. *Int J Cancer* 2021, 149: 169–176
- Deng Y, Zhao P, Zhou L, Xiang D, Hu J, Liu Y, Ruan J, *et al.* Epidemiological trends of tracheal, bronchus, and lung cancer at the global, regional, and national levels: a population-based study. *J Hematol Oncol* 2020, 13: 98
- Zhou YP, Yang M, Yao PT, Ge YB, Li N. Quality assessment of guidelines and consensus in lung cancer chemotherapy. *Zhonghua Zhong Liu Za Zhi* 2020, 42: 1025–1033
- Bezzecchi E, Ronzio M, Semeghini V, Andrioletti V, Mantovani R, Dolfini D. NF-YA overexpression in lung cancer: LUAD. *Genes* 2020, 11: 198
- Aguilar-Serra J, Gimeno-Ballester V, Pastor-Clerigues A, Milara J, Marti-Bonmati E, Trigo-Vicente C, Alós-Almiñana M, *et al.* Osimertinib in first-line treatment of advanced EGFR-mutated non-small-cell lung cancer: a cost-effectiveness analysis. *J Comp Eff Res* 2019, 8: 853–863
- Hoischen C, Yavas S, Wohland T, Diekmann S. CENP-C/H/I/K/M/T/W/N/L and hMis12 but not CENP-S/X participate in complex formation in the nucleoplasm of living human interphase cells outside centromeres. *PLoS ONE* 2018, 13: e0192572
- Basilico F, Maffini S, Weir JR, Prumbaum D, Rojas AM, Zimniak T, De Antoni A, *et al.* The pseudo GTPase CENP-M drives human kinetochore assembly. *eLife* 2014, 3: e02978
- Sui X, Han X, Chen P, Wu Q, Feng J, Duan T, Chen X, *et al.* Baicalin induces apoptosis and suppresses the cell cycle progression of lung cancer cells through downregulating Akt/mTOR signaling pathway. *Front Mol Biosci* 2021, 7: 602282
- Wu ZH, Yang DL. High CENPM mRNA expression and its prognostic significance in hepatocellular carcinoma: a study based on data mining. *Cancer Cell Int* 2020, 20: 406
- Xiao Y, Najeeb RM, Ma D, Yang K, Liu Q. Upregulation of CENPM promotes hepatocarcinogenesis through multiple mechanisms. *J Exp Clin Cancer Res* 2019, 38: 458
- Zou Y, Sun Z, Sun S. LncRNA HCG18 contributes to the progression of hepatocellular carcinoma via miR-214-3p/CENPM axis. *J Biochem* 2020, 168: 535–546
- Maiato H, Gomes AM, Sousa F, Barisic M. Mechanisms of chromosome congression during mitosis. *Biology* 2017, 6: 13
- Haley CO, Waters AM, Bader DM. Malformations in the murine kidney caused by loss of CENP-F function. *Anat Rec* 2019, 302: 163–170
- Tovini L, McClelland SE. Impaired CENP-E function renders large chromosomes more vulnerable to congression failure. *Biomolecules* 2019, 9: 44
- Jeffery D, Gatto A, Podsypanina K, Renaud-Pageot C, Ponce Landete R, Bonneville L, Dumont M, *et al.* CENP-A overexpression promotes distinct fates in human cells, depending on p53 status. *Commun Biol* 2021, 4: 417
- Liu Y, Yu W, Ren P, Zhang T. Upregulation of centromere proteinM promotes tumorigenesis: a potential predictive target for cancer in humans. *Mol Med Rep* 2020, 22: 3922–3934
- Zhang J, Hu J, Li W, Zhang C, Su P, Wang Y, Sun W, *et al.* Rapamycin antagonizes BCRP-mediated drug resistance through the PI3K/Akt/mTOR signaling pathway in mPR α -positive breast cancer. *Front Oncol* 2021, 11: 608570
- Wang P, Hu Y, Qu P, Zhao Y, Kong B. PTPRZ1 inhibits the cisplatin resistance of ovarian cancer by regulating PI3K/AKT/mTOR signal pathway. *Bmc Cancer* 2020, 36: 845–852
- Yan X, Wu S, Liu Q, Zhang J. RRS1 promotes retinoblastoma cell proliferation and invasion via activating the Akt/mTOR signaling pathway. *Biomed Res Int* 2020, 2020: 1–10
- Ni Z, Sun W, Li R, Yang M, Zhang F, Chang X, Li W, *et al.* Fluorochloridone induces autophagy in TM4 Sertoli cells: involvement of ROS-mediated AKT-mTOR signaling pathway. *Reprod Biol Endocrinol* 2021, 19: 64
- Zhao L, Zhu L, Oh YT, Qian G, Chen Z, Sun SY. Rictor, an essential component of mTOR complex 2, undergoes caspase-mediated cleavage during apoptosis induced by multiple stimuli. *Apoptosis* 2021, 26: 338–347
- Pei XD, Yao HL, Shen LQ, Yang Y, Lu L, Xiao JS, Wang XY, *et al.* α -Cyperone inhibits the proliferation of human cervical cancer HeLa cells via ROS-mediated PI3K/Akt/mTOR signaling pathway. *Eur J Pharmacol* 2020, 883: 173355
- Hong X, Hong X, Zhao H, He C. Knockdown of SRPX2 inhibits the proliferation, migration, and invasion of prostate cancer cells through the PI3K/Akt/mTOR signaling pathway. *J Biochem Mol Toxicol* 2019, 9: e22237
- Zheng C, Zhang T, Li D, Huang C, Tang H, Ni XF, Chen B. Upregulation of CENPM facilitates tumor metastasis via the mTOR/p70S6K signaling pathway in pancreatic cancer. *Oncol Rep* 2020, 44: 1003–1012